Aquatic Geochemistry (2022) 28:27–42
https://doi.org/10.1007/s10498-021-09402-5

ORIGINAL ARTICLE

A Late Holocene Record of Variations in the Chemical Weathering Intensity and Pedogenesis in a Lake Catchment from Southern India

Kizhur Sandeep[1,2] · **Rajasekhariah Shankar**[1,3] · **Anish Kumar Warrier**[1,4]

Received: 29 May 2021 / Accepted: 29 November 2021 / Published online: 11 January 2022

Abstract
We investigated the detrital influx, chemical weathering intensity, provenance and pedogenesis over the past 2,500 years in the catchment of Pookot Lake, southern India. The down-core variations of metal/Al ratios (Na/Al, K/Al, Mg/Al, Ca/Al, Fe/Al, Mn/Al, Zn/Al, Ba/Al) of the Pookot sediments indicate changes in the rainfall-induced terrigenous inflow to the lake. In contrast, fluctuations in the chemical index of alteration (CIA) and Rb/Sr values denote the variability in the strength of chemical weathering in the watershed of the lake. The results show that the detrital influx, and hence rainfall, remained steady except during 1500–600 cal. years B.P. (high) and 600–300 cal. year B.P. (low) in the Pookot lake catchment. However, the periods of high/low chemical weathering intensity in the catchment do not correspond to periods of high/low detrital influx to the lake basin. The similar shale-normalized rare earth elemental curves point to a uniform provenance. The past pedogenic activity is indicated by pedogenic χ_{lf} and pedogenic χ_{fd} derived from citrate-bicarbonate-dithionite (CBD) extraction. The data indicate that the fine-grained magnetite/maghemite formed during the pedogenesis mainly contributes to the magnetic signal of sediments. The degree of pedogenesis was strong during 2500–2000 cal. years B.P. and moderate throughout 1500–600 cal. years B.P. The pedogenic intensity became stronger again during ~ 600 cal. years B.P., which weakened between 600 and 300 cal. years B.P. and remained steady thereafter. The present study indicates that detrital influx proxies like metal/Al ratios are more suitable for reconstructing past climate in tropical climate rather than chemical weathering indices.

Keywords Chemical weathering · Detritus influx · Southern India · Pedogenesis · Monsoon

✉ Kizhur Sandeep
sandeepk01@gmail.com

[1] Department of Marine Geology, Mangalore University, Mangalagangotri 574 199, India

[2] Present Address: Department of Geology, School of Earth Science Systems, Central University of Kerala, Periye (P.O.), Tejaswini Hills, Kasaragod, Kerala 671320, India

[3] No. 29, 4th Main, Chamarajapete, Bengaluuru, Karnataka 560 018, India

[4] Present Address: Centre for Climate Studies / Department of Civil Engineering (Manipal Institute of Technology), Manipal Academy of Higher Education, Manipal, Karnataka 576104, India

1 Introduction

The indiSediments from the Arabiances of chemical weathering of lake sediments have been used widely for deciphering past environment and fluctuations in Asian monsoon in semi-arid (Liu et al. 2014; Ao et al. 2010; Jin et al. 2006) and temperate (Sun et al. 2018; Xu et al. 2016; An et al. 2011) regions. In the Indian context, relationship between sediment geochemistry and climate is well established in lakes from Himalayan region (Shah et al. 2021; Lone et al. 2020; Shah et al. 2020a, Shah et al. 2020b; Babeesh et al. 2019; Bhushan et al. 2018) and north-western India (Sinha et al., 2006; Banerji et al., 2021). Sediments from the Arabian Sea and Bay of Bengal also indicate a climate-silicate weathering link on long time scales of glacial-interglacial periods (Miriyala et al. 2017). However, only a few studies have been directed at lacustrine sediments of southern India to establish chemical weathering-rainfall linkage (Rajmanickam et al. 2017; Warrier and Shankar 2009). Besides, a few investigations of lake sediments have focussed on source area weathering and provenance (Nair and Achyuthan 2017; Babeesh et al. 2018; Gopal et al. 2020). Chemical weathering under high rainfall conditions in tropical regions leads to intense leaching of cations and silica (Formoso 2006). The intensity of chemical weathering varies both temporally and spatially in response to climate change. Hence, it is imperative to assess whether chemical weathering parameters can be used to reconstruct past climate on short time scales in a small catchment (Liu et al. 2014). The response time of chemical weathering to subtle changes in rainfall during the Holocene and climate-driven thresholds for chemical weathering in tropical high rainfall conditions of southern India also need to assessed.

The present study focuses on the relationship between chemical weathering, soil formation and monsoon-induced erosion in surrounding watershed of Pookot Lake, located in the south-western part of India. The findings of this investigation may help in assessing the response of a particular geochemical proxy to climate change and evaluating a suitable chemical weathering proxy for palaeomonsoonal reconstruction under tropical climate. Warrier and Shankar (2009) documented a positive relationship between rainfall and intensity of chemical weathering as interpreted from metal/Al ratios of Thimmannanayakanakere sediments in Karnataka (Fig. 1). The Mg/Al ratio and CIA (chemical index of alteration) of Ennamangalam Lake sediments, Tamil Nadu (Fig. 1), do respond to hydrological and precipitation changes (Mishra et al. 2019). Similarly, chemical weathering indices in sediment cores from Kukkal Lake (Fig. 1) indicated intense weathering in response to rainfall (Rajmanickam et al. 2017). However, rainfall in the catchments of these three lakes is not high (~ 1500 mm or less) compared to that in the south-western part of India along the Western Ghats (~ 3500 mm). The Pookot Lake in Wayanad District of Kerala is situated in such a rainfall regime and is ideal to assess the geochemical response and pedogenesis under a tropical monsoon climate. Earlier studies on Pookot Lake sediments based on environmental magnetism (Sandeep et al. 2015) and pollen (Bhattacharya et al. 2015) indicated that the region experienced three broad climatic shifts in the past 3000 years. These three phases are 3100–2500 cal. years B.P. (strong monsoon), 2500–1000 cal. years B.P. (low but steady monsoon) and 1000 cal. years B.P. to the present (shift towards strong monsoonal conditions). In the present study, various metal/Al ratios and indices of chemical weathering (chemical index of alteration and Rb/Sr ratio) have been employed to assess detrital influx and chemical weathering intensity in the lake watershed. The changes in source area weathering and provenance of sediments have been evaluated using rare earth elemental (REE) data. We have also employed citrate-bicarbonate-dithionite (CBD)

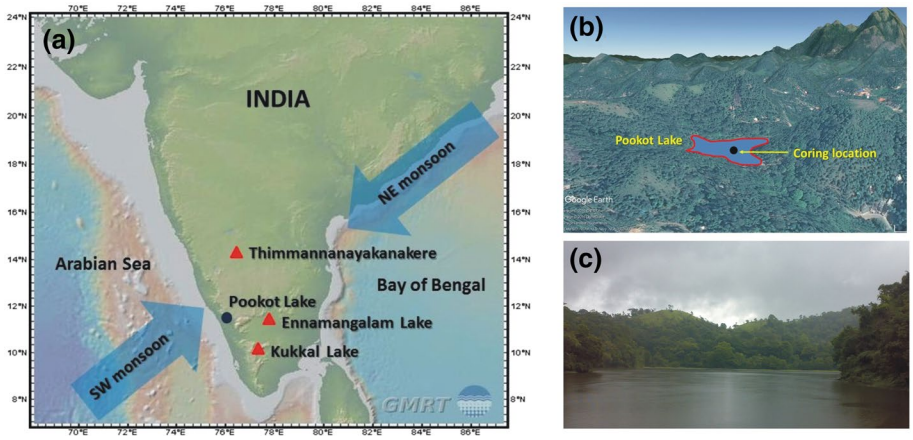

Fig. 1 Location map of the Pookot Lake: **a** geographical location of the study area (source: https://www.gmrt.org/GMRTMapTool/); **b** satellite image of the lake and its watershed (source: Google Earth) with the coring location shown with a black dot; and **c** photograph of the lake and the surrounding vegetation

extraction procedure (Warrier and Shankar 2009; Mehra and Jackson 1960) to assess the proportion of pedogenic iron oxide minerals in sediments which infer the degree of pedogenesis in the Pookot catchment.

2 Study Area

Pookot Lake (PK) is an elliptical, closed, fresh water lake located in the inter-montane region near Vythiri in north-eastern Kerala (Fig. 1). It is situated at a height of 775 m above mean sea level and covers an area of ~ 0.09 sq. km.; water depth varies from 6 to 7 m. Hornblende-biotite gneiss and charnockite are the main parent rocks in the lake catchment (Sandeep et al. 2015). These rocks are overlain by ferruginous forest loamy soil (Kerala Forest Department 1986). The region experiences tropical monsoon climate (Am) as per Koppen climatic classification. It receives a mean yearly rainfall of 384 cm and temperature of 23.2 °C (https://en.climate-data.org/).

3 Materials and Methods

3.1 Sampling and Chronology

The core sample from Pookot Lake (2.2 m) was taken from the deep part of the lake by inserting a pipe (diameter of 3.8 cm and length 10 m) made up of polyvinyl chloride. The pipe was split longitudinally into two halves in the laboratory and sub-sampled at an interval of 5 mm. Organic matter of sediment samples was used for C-14 dating by accelerator

mass spectrometry. Further details of sampling and ^{14}C analysis are given by Sandeep et al. (2015).

3.2 Inorganic Geochemical Analysis

Finely powdered samples (n = 26) were heated with an acid mixture (concentrated HNO_3, HF, $HClO_4$) in Teflon beakers and digested. The dried residue was heated to ~ 110 °C after adding $HClO_4$ and HF. This produced a crystalline paste, which was dissolved in 5 ml HCl. The undigested particles were filtered and removed using a filter paper. Deionized water was added to the filtrate making it up to a volume of 50 ml. Inductively coupled plasma mass spectrometers were used to analyse major element (Thermo Fisher X-Series II) and trace element (PerkinElmer Sciex ELAN DRC II) concentrations. Two geochemical standards, namely SCo-1 and MAG-1 (USGS 1995), were employed to examine the accuracy (< 5%). The precision was inside acceptable limits (< 1% and 5% for major and trace elements, respectively).

3.3 Citrate-Bicarbonate-Dithionite (CBD) Analysis

The method proposed by Mehra and Jackson (1960) was employed for extracting secondary iron oxides from ten sediment samples. Four grams of the sample was disaggregated and added into a centrifuge tube with sodium citrate (0.3 M) and sodium bicarbonate solution. The suspension was heated at 75 °C using a water bath after the addition of sodium dithionite. The sample mixture was centrifuged, and the supernatant solution was transferred to another bottle. The filtrate was dried at 35 °C. The sediments were subjected to a four-step CBD treatment, and their magnetic susceptibility (χ_{lf}) values were determined after the completion of each step. Pre- and post-CBD χ_{lf} values were measured using a Bartington Susceptibility Meter.

4 Results

The elemental concentrations in the sediment core decrease in the sequence: Fe, Al, K, Mg, Ti, Ca, Na, P, Ba, Zn, Sr, Cu, Pb and Rb. However, we could not measure the abundance of Si and O in the samples. The concentration of Al in the samples varies between 0.9% and 14.9% (mean = 6%). Elements like K, Na, Mg, Ca, Ti, Cu and Rb exhibit a positive correlation with Al (Supplementary Table 1). This indicates their supply from a common source (Pattan et al. 2005). However, Fe, Mn and P exhibit a negative correlation with Al. Higher Fe content in comparison with Al may be due to the weathering of laterites present in the lake's catchment. Most of the metal/Al ratio values exhibit low but steady values except for the phase 1500 to 300 cal. years B.P. when significant changes are documented (Fig. 2). As Sr/Al, Cu/Al, Rb/Al, P/Al and Pb/Al values also exhibit a similar trend, they are not plotted. All the metal/Al ratio values exhibit statistically significant positive correlations amongst themselves (Table 1), except for Ti/Al which is negatively correlated with other metal/Al values. The past 2500 years period can be divided into four distinct 'geochemical phases': GP1 (2500–1500 cal. years B.P.), GP2 (1500–600 cal. years B.P.), GP3 (600–300 cal. years B.P.) and GP4 (300 cal. years B.P. to present) based on variations in geochemical ratios (Fig. 2). The values of

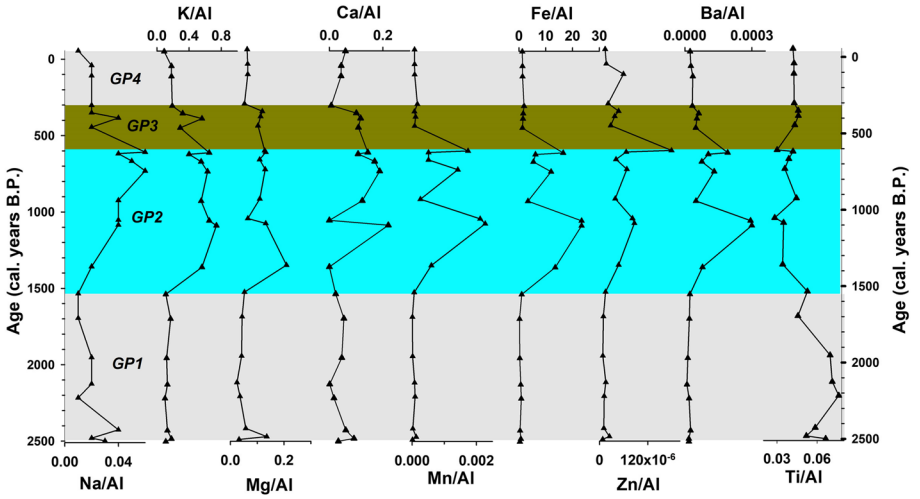

Fig. 2 Down-core variations of Al-normalized elemental concentrations. Most of the metal/Al ratio values, except Ti/Al, exhibit similar down-core behaviour with an increasing trend during the phase GP2 and decreasing trend during GP3

chemical index of alteration (CIA) range from 60.1 to 92.6% (average = 79.2%; Fig. 3). The down-core variations exhibited by CIA and Rb/Sr values are opposite to what is exhibited by metal/Al values (Fig. 3).

GP1 (2500–1500 cal. years B.P.) A small peak at ~ 2500 cal. years B.P. is documented for Na/Al, Mg/Al, Ca/Al and Ti/Al. The values remain low and steady thereafter, except for Ti/Al which exhibits high values. Chemical weathering proxies like Rb/Sr and CIA register steady values.

GP2 (1500–600 cal. years B.P.) The Zn/Al, Ba/Al, Ca/Al, K/Al, Mn/Al, Na/Al, Fe/Al and Mg/Al values show an increasing trend (Fig. 2). However, Rb/Sr and CIA display a decreasing trend.

GP3 (600–300 cal. years B.P.) Zn/Al, Ba/Al, Ca/Al, K/Al, Mn/Al, Na/Al, Fe/Al and Mg/Al values display a decreasing trend. Rb/Sr and CIA values increase during this phase.

GP4 (300 cal. years B.P. to Present) The metal/Al values exhibit a low but steady trend during this phase, similar to that of the GP1 phase. The Rb/Sr and CIA values are constant in this phase.

Rare earth elements reveal identical flat shale-normalized patterns (with values < 1; Fig. 4). The various REE ratios like $(LREE/HREE)_N$, $(La/Yb)_N$, $(Gd/Yb)_N$ and $(La/Sm)_N$ exhibit values ranging between 0.70 and 1.47 with mean values close to one. Eu anomaly values vary between 1.23 and 1.50 (mean = 1.37), whereas Ce anomaly varies between 1.07 and 1.57 (mean = 1.26). All the REE's investigated display similar down-core variations (Fig. 5) with high 'r' values among themselves (Supplementary Table 2). The down-core variations of REE's are similar to those of Al_2O_3, Rb, Rb/Sr and CIA % with high values during the period 2400–1500 cal. years B.P.

The CBD extraction procedure was carried out on ten sediment samples with different initial magnetic susceptibility values. Following the first step of CBD extraction, the initial susceptibility values decreased (4% to 93%; average = 40%; Fig. 6). There was an average of 74% decrease in χ_{lf} values after the fourth step.

The pedogenic χ_{lf} and pedogenic χ_{fd} are calculated as below (Vidic et al. 2000):

Table 1 Correlation matrix for metal/Al ratios of Pookot Lake sediment samples

	Fe/Al	Mn/Al	Zn/Al	Pb/Al	Ba/Al	Cu/Al	Na/Al	K/Al	Mg/Al	Ca/Al	Ti/Al	P/Al	Rb/Al	Sr/Al
Fe/Al	1.00													
Mn/Al	**0.97**	1.00												
Zn/Al	**0.74**	**0.78**	1.00											
Pb/Al	**0.81**	**0.80**	**0.83**	1.00										
Ba/Al	**0.96**	**0.97**	**0.74**	**0.84**	1.00									
Cu/Al	**0.94**	**0.92**	**0.79**	**0.92**	**0.95**	1.00								
Na/Al	**0.58**	**0.66**	**0.70**	**0.57**	**0.60**	**0.59**	1.00							
K/Al	**0.82**	**0.80**	**0.73**	**0.73**	**0.80**	**0.85**	**0.79**	1.00						
Mg/Al	*0.52*	0.41	**0.52**	**0.56**	0.42	**0.60**	**0.54**	**0.75**	1.00					
Ca/Al	0.34	*0.45*	*0.47*	0.39	*0.44*	0.41	**0.74**	**0.63**	*0.50*	1.00				
Ti/Al	**−0.64**	**−0.61**	**−0.63**	**−0.76**	**−0.63**	**−0.73**	*−0.51*	**−0.70**	**−0.64**	−0.41	1.00			
P/Al	**0.81**	**0.87**	**0.57**	**0.63**	**0.85**	**0.81**	**0.67**	**0.74**	*0.45*	**0.64**	**−0.53**	1.00		
Rb/Al	**0.83**	**0.78**	**0.80**	**0.79**	**0.77**	**0.87**	**0.71**	**0.94**	**0.80**	*0.49*	**−0.75**	**0.65**	1.00	
Sr/Al	**0.94**	**0.96**	**0.76**	**0.83**	**0.98**	**0.93**	**0.68**	**0.83**	*0.50*	**0.57**	**−0.64**	**0.87**	**0.81**	1.00

Values in bold exhibit a statistical significance (p) values < 0.01 and those in italics have p values < 0.05

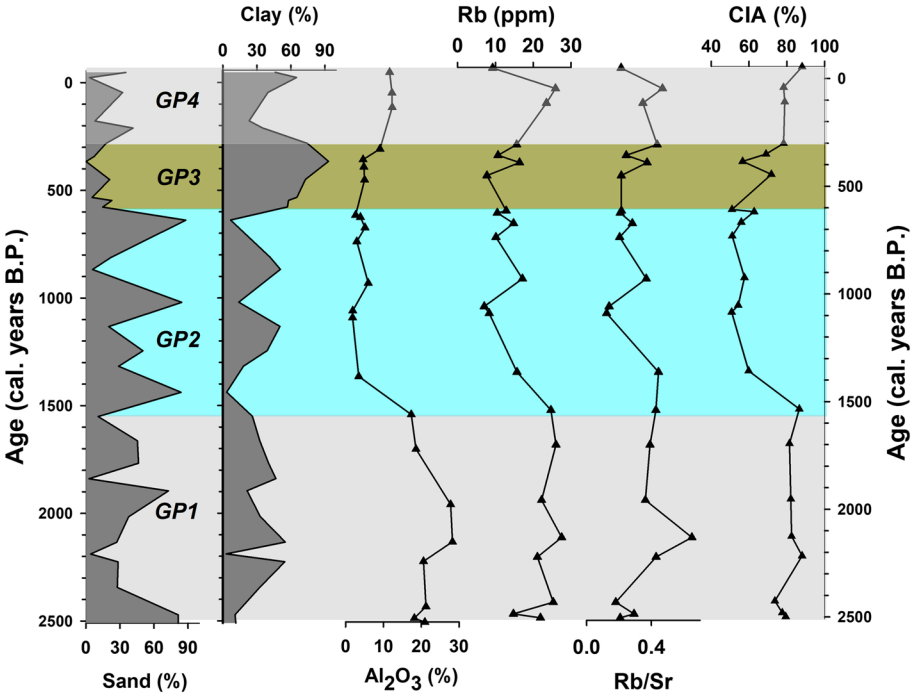

Fig. 3 Down-core variations of sand %, clay %, Al_2O_3, Rb, Rb/Sr ratio and chemical index of alteration (CIA). Note their reverse trend compared to that of metal/Al ratio values (the sand and clay percentage data from Bhattacharyya et al. 2015)

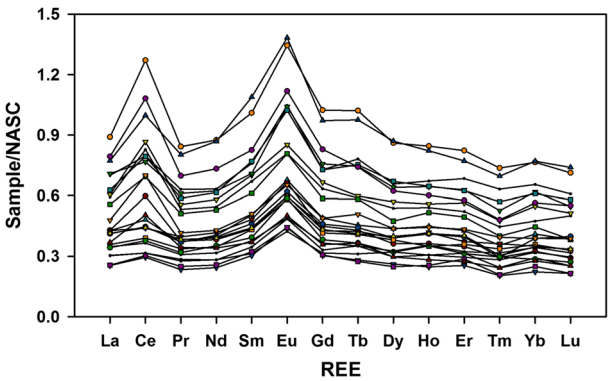

Fig. 4 Shale-normalized rare earth element (REE) patterns for Pookot Lake sediment samples. Note their similarity, which points to a constant source region of sediments

$$Pedogenic\,\chi_{lf} = \left(pre - CBD\,\chi_{lf}\right) - \left(post - CBD\,\chi_{lf}\right)$$

$$Pedogenic\,\chi_{fd} = \left(pre - CBD\,\chi_{fd}\right) - \left(post - CBD\,\chi_{fd}\right)$$

The three samples exhibiting high initial χ_{lf} values (Nos. 11, 13, 14) show a reduction of about 89% after the extraction. The average initial susceptibility values of these samples declined from an average of 108 to 11 ($\times 10^{-8}$ m^3 kg^{-1}; Fig. 6). Sediment samples with

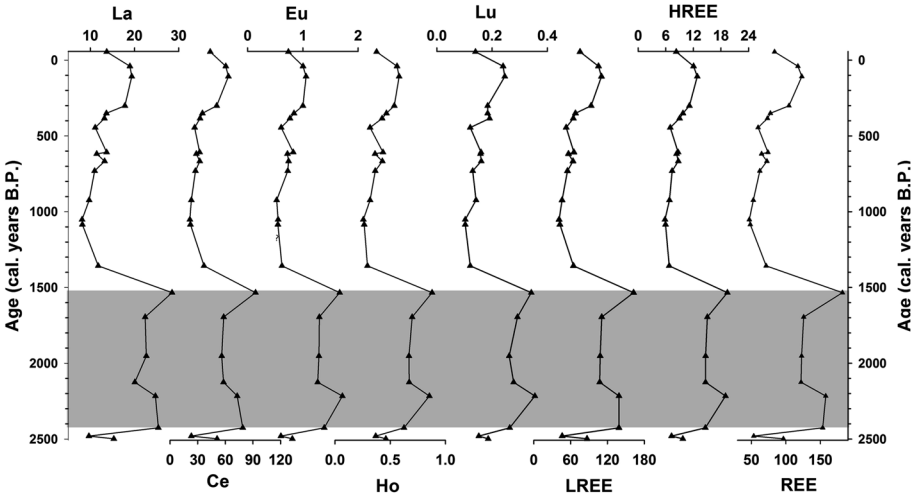

Fig. 5 Variations of rare earth element (REE) concentrations (in ppm) in Pookot Lake sediment samples of the past 2500 years. Note the high values during the 2400–1500 cal. years B.P. period

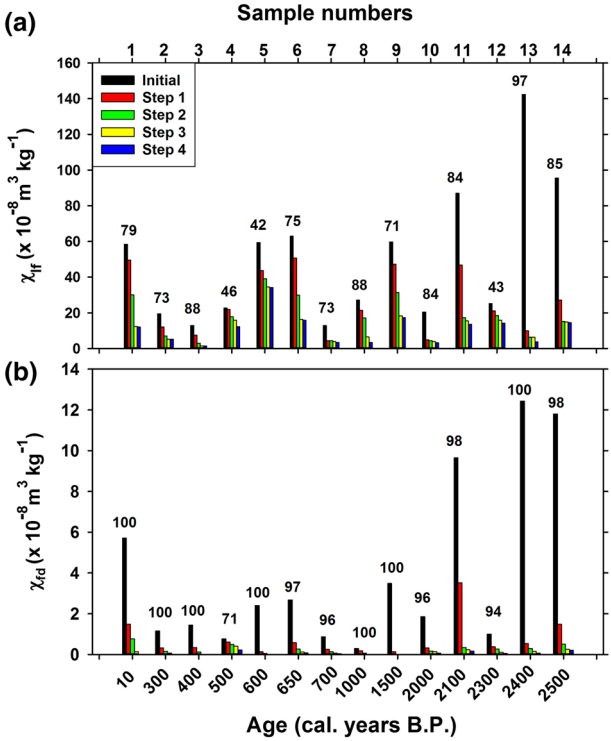

Fig. 6 Magnetic parameter data obtained during the four-step CBD treatment for select samples of Pookot Lake sediments. **a** Magnetic susceptibility (χ_{lf}); **b** frequency-dependent magnetic susceptibility (χ_{fd}). The values above every bar group denote the decline (in percentage) in χ_{lf} or χ_{fd} after the fourth step of treatment

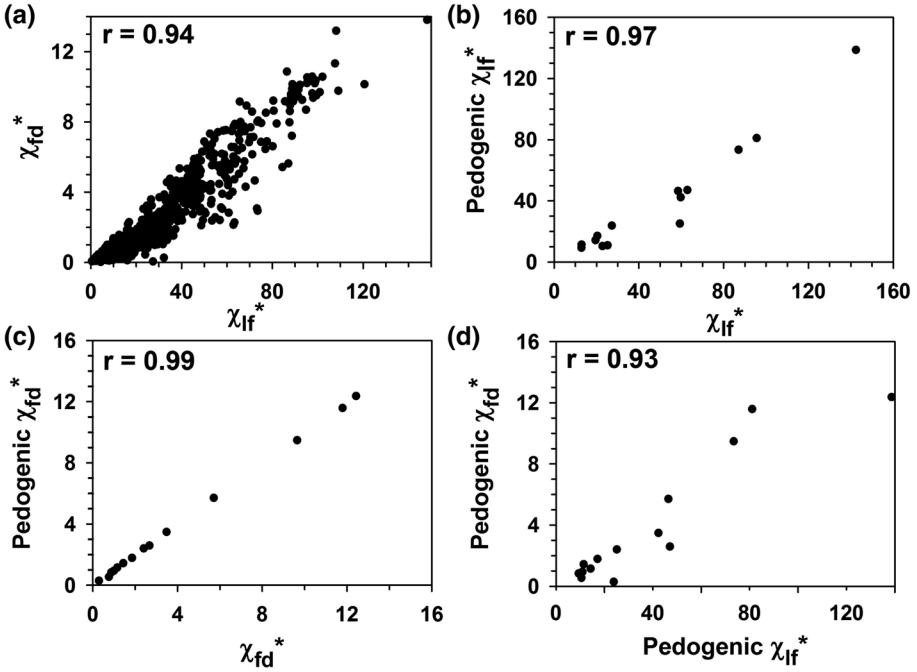

Fig. 7 Biplots of magnetic parameter values. **a** χ_{lf} *vs.* χ_{fd}; **b** pedogenic χ_{lf} *vs.* χ_{lf}; **c** χ_{fd} vs. pedogenic χ_{fd} **d** pedogenic χ_{lf} *vs.* pedogenic χ_{fd} ($p < 0.01$ level; * units of 10^{-8} m^3 kg^{-1})

initial low χ_{lf} values (Nos. 2, 3, 4, 7, 8, 10 and 12) exhibit a decrease of 71% (93×10^{-8} m^3 kg^{-1} to 15×10^{-8} m^3 kg^{-1}), which is only marginally low compared to the high-χ_{lf} samples. The initial pre-CBD χ_{fd} values decreased from an average of 4 to 0.02 ($\times 10^{-8}$

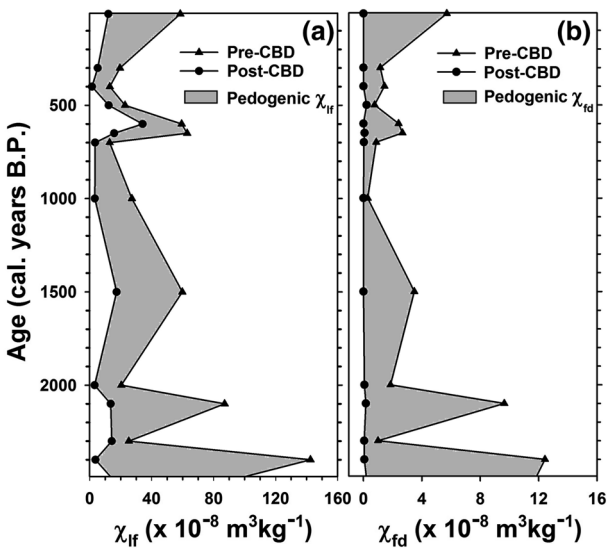

Fig. 8 Down-core variations of pedogenic χ_{lf} and pedogenic χ_{fd} in PK sediments during the past 2500 years

$m^3\ kg^{-1}$). A similar trend is also exhibited by frequency-dependent susceptibility. Pedogenic χ_{lf} values exhibit very high correlation coefficient values like 0.97 and 0.93 with χ_{lf} and pedogenic $\chi_{fd,}$ respectively (Fig. 7). Between themselves, χ_{fd} and pedogenic χ_{fd} are strongly correlated with a correlation coefficient of 0.99. The pedogenic χ_{lf} and pedogenic χ_{fd} values exhibit significant down-core variations (Fig. 8). The pedogenic χ_{lf} values range from 9.4 to $139\times10^{-8}\ m^3\ kg^{-1}$, whereas pedogenic χ_{fd} values range between 0.3 and 12.4 ($\times10^{-8}\ m^3\ kg^{-1}$).

5 Discussion

5.1 Chemical Weathering and Catchment Erosion

Ratios like Mg/Al, K/Al, Fe/Al and Na/Al are effective indicators of detrital input (Sun et al. 2008; Wei et al. 2006; Bertrand et al. 2012). A high rainfall would lead to increased soil erosion in the catchment, resulting in high contents of these elements in lake sediments (Mackereth 1966). Elements such as Ca, Na, K, Mg and Sr that are derived from chemical weathering as a result of heavy precipitation are more soluble and mobile (Mackereth, 1966; Mischke and Zhang 2010; Sun et al. 2010). On the contrary, Al is commonly a terrestrial element which is insoluble and resistant under oxic and anoxic conditions (Zhong et al. 2012; Brown et al. 2000). During periods of increased chemical weathering, surface water of lakes becomes enriched in these mobile elements. The increase in stream- and overland-water flow into the lake results in a higher total content of these elements in lake sediments (Minyuk et al. 2014). Normalization to Al was carried out in the present study to account for the variable dilution in the element records and to evaluate chemical solution, hydrolysis and migration relative to Al (Zhong et al. 2012). The extreme chemical weathering of mica and feldspars would lead to high values of Na/Al and K/Al in lacustrine sediments (Felton et al. 2007). Although these metal/Al ratios of sediments are predominantly used in lakes situated under sub-tropical to semi-arid climates (Minyuk et al. 2014; Bertrand et al. 2012; Zhong et al. 2012), they have also been employed in lakes with tropical climate (Warrier and Shankar 2009; Rajmanickam et al. 2017; Veena et al. 2014). Hence, higher ratios in PK lake sediments should indicate the relative variations in soluble and mobile element input to the lake as a result of strong chemical weathering and vice versa.

As most of the metal/Al ratios exhibit similar down-core variations and significantly correlated among themselves (Fig. 2; Table 1), it can be argued that they possess identical detrital origin and came from silicate fraction. The CIA values indicate intermediate to extreme silicate weathering in the lake catchment. We assume that the CaO content of the sediments came from the silicate fraction only, because of the absence of carbonate rocks in the surrounding area, the low $CaCO_3$ content in sediments (average = ~ 5%; Sandeep et al. 2015) and the high correlation of Ca/Al with other metal/Al ratios like Na/Al and K/Al (Table 1). Even after re-calculating the CIA values by adopting the CaO content of silicate fraction, the down-core variations of the former remain unchanged.

Detrital input to the lake increased during GP2 (between 1500 and 600 cal. BP), but decreased subsequently, i.e. during GP3 (between 600 and 300 cal. BP) and remained steady during GP1 (2500–1500 cal. years B.P.) and GP4 (300 cal. years B.P. to Present) (Figs. 2 and 3). The increased rainfall in the Pookot Lake catchment as indicated by higher terrigenous input is evident during 1500–600 cal. years B.P (Fig. 2). This may be due to high rainfall which led to an increase in catchment erosion. The rainfall reduced during the

600–300 cal. years B.P. phase and remained uniform afterwards (Fig. 2). The rainfall was slow but steady before 1500 cal. years B.P. excluding a small peak at ~ 2500 cal. years B.P. as exhibited by some metal/Al ratios. However, the chemical weathering intensity does not follow this trend. In fact, periods of high detrital influx are characterized by low chemical weathering intensity as denoted by the low CIA and Rb/Sr ratio values and vice versa (Fig. 3). Hence, periods of high chemical weathering intensity in the catchment do not correspond to periods of high detrital influx to the lake basin and vice versa. There may be two reasons for this: (1) the lag in geochemical response to a particular climatic event, and (2) variations in chemical weathering indices may, in fact, be controlled by the influx of terrigenous clay-sized particles. Investigations of arid to semi-arid regions in southern China have revealed that high rainfall and the resulting increased intensity of chemical weathering led to enrichment of lake surface water in elements with high mobility (Sr, K, Ca, and Na). In this context, low CIA, CIW, PIA, and Rb/Sr values indicate a high intensity of chemical weathering and vice versa (Minyuk et al. 2014; Sun et al. 2018). As per Liu et al. (2014), "CIA was primarily employed to evaluate the intensity of in situ weathering". This original interpretation is reversed when applied to lacustrine sediments because with increased chemical weathering, labile elemental oxides (like Na_2O, K_2O and CaO) are easily carried to lakes, decreasing the CIA (An et al. 2011). Hence, high oxide percentages and metal/Al ratios along with low Rb/Sr and CIA values may be indicative of a high degree of chemical weathering (Liu et al. 2014). A similar explanation was offered for Lake Xingkai (Sun et al. 2018), Daihai Lake (Jin et al. 2001a, b), Heqiong Paleolake (An et al. 2011) and Barkol Lake (Zhong et al. 2012). Earlier studies (Sandeep et al. 2015; Bhattacharya et al. 2015) have indicated that the period 2500–1000 cal. years B.P. was typified by low magnetic susceptibility values and absence of pollen grains, indicating the drying of the lake. The period 1000–600 cal. years B.P. was exemplified by a high pollen percentage, which decreased between 600 and 300 cal. years B.P. (Bhattacharyya et al. 2015). Bhattacharyya et al. (2015) also documented a high proportion of sand and a low proportion of clay during GP2 but the opposite during GP3 (Fig. 3).

Periods of high (low) pollen abundance and increased vegetation in the catchment correspond to high (low) metal/Al ratio values in sediment. In such a scenario, chemical weathering indices like CIA and Rb/Sr ratio of sediments weathered significantly in a tropical climate may not be suitable for the reconstruction of chemical weathering intensity/rainfall in the catchment. The geochemical parameters indicative of detrital influx may be more apt for tropical regions like the south-western part of India to reconstruct past rainfall. Phases GP2 and GP3 may correspond, respectively, to the Medieval Climatic Anomaly (with high rainfall) and the Little Ice Age (with low rainfall). However, signatures of these two short climatic events are not well documented in the southern India (Mishra et al. 2019; Basu et al. 2017; Veena et al. 2014) except by Warrier et al. (2017).

5.2 Provenance

Variations in REE's may be used for provenance studies because of their low mobility during weathering and transportation (Das and Haake 2003). The identical, flat shale-normalized REE patterns (with values < 1; Fig. 4) suggest invariable source rocks and provenance during the past 2500 years (McLennan 1989). Fractionation among LREE's and HREE's as well as between them is insignificant. The persistence of the same REE pattern in all the samples indicates that the source lithology has not varied much during the past two millennia. Also, the REE distribution is not affected by weathering (McLennan 1989) during the

past 2500 years. The REE signature may have been derived from gneissic and charnockitic rocks in the catchment.

All the REE's investigated have a close relationship and point to a common provenance as REEs are not affected by chemical changes during their transportation from source area to lake basin (Fleet 1984). They also show similar down-core variations as do Al_2O_3, Rb, Rb/Sr and CIA % with high values during the 2400–1500 cal. years B.P. period (Fig. 5). Further, clay percentage and Al content are also high during this period. The REE values are high during GP1 but low during GP2. This may be because rare earth elements are usually concentrated in the clay portion. This statement is corroborated by the good correlation (r = 0.72) between ΣREE and Al.

5.3 Pedogenesis in the Catchment Area

The intensity of pedogenesis in a lake catchment is estimated based on the proportions of lithogenic and pedogenic iron minerals in sediments determined using citrate–bicarbonate–dithionite extraction procedure. The procedure dissolves and extracts fine grained magnetite/maghemite and haematite, whereas the coarse grained lithogenic component remains unaffected (Vidic et al. 2000). According to Maher and Thompson (1991), the palaeorainfall signal is associated mainly with the pedogenic constituent of sediments. In this study, pedogenic χ_{lf} and pedogenic χ_{fd} have been employed to assess the proportion of pedogenic constituent in the bulk susceptibility values. The technique was applied on Thimmannanayakanakere Lake (situated in Chitradurga, Karnataka) sediments by Warrier and Shankar (2009) who proposed that the amount of fine-grained magnetite produced in soils is directly related to the amount of rainfall in the catchment.

The CBD data indicate that χ_{lf} is dominated by the CBD-extractable fraction and that fine-grained pedogenic magnetite/maghemite makes a significant contribution to the magnetic signal of PK sediments. The influence of lithogenic grains is low even in the initial low-χ_{lf} samples. The strong correlations documented between pedogenic χ_{lf} and χ_{lf} and pedogenic χ_{fd} (Fig. 7) confirm that the magnetic properties of Pookot sediments are mainly influenced by the pedogenic magnetic minerals produced during soil formation. Periods of high production of pedogenic magnetite in the lake catchment are typified by high values of pedogenic χ_{lf} and pedogenic χ_{fd} and vice versa. Ultra-fine grained pedogenic magnetite may be inorganically produced in situ (Maher and Taylor 1988; Taylor et al. 1987) during alternate wetting and drying cycles in soils (Dearing et al. 1996). The production of fine grained pedogenic magnetic minerals depends on the intensity of chemical weathering and the degree of pedogenesis in the catchment. Previous studies have demonstrated that magnetic minerals with a coarse grain size (MD) are transformed into secondary magnetic minerals with a fine gran size (SP and SSD) during pedogenesis in the lateritic soils of southern India (Ananthapadmanabha et al. 2014; Sandeep et al. 2012; Amrutha et al. 2021).

The 2500–2000 cal. years B.P. period (GP1) was typified by a high degree of pedogenesis as indicated by peaks in pedogenic χ_{lf} and χ_{lf} (Fig. 8). Phase GP2 exhibits moderate values though fluctuating. High values are displayed at ~ 600 cal. years B.P., which decrease within a short span of 300 years (600 to 300 cal. years B.P.; Phase GP3; Fig. 8). The degree of pedogenesis revealed by pedogenic magnetite corresponds to what is suggested by the metal/Al ratios as well.

6 Conclusions

The conclusions we drew from the geochemical and CBD analyses of Pookot Lake sediments are:

- A high detrital influx is documented during the period 1500–600 cal. years B.P., which decreased between 600 and 300 cal. year B.P. This indicates that the rainfall was, respectively, high and low during those periods, but it was, by and large, steady during the Late Holocene.
- Periods of high/low chemical weathering intensity in the catchment do not correspond to those of high/low detrital influx to the lake. Such a mismatch may be due to a longer response time of chemical weathering to climatic changes and/or terrigenous clay-sized particles influencing chemical weathering indices.
- Pedogenesis was strong during 2500–2000 cal. years B.P. and moderate from 1500 to 600 cal. years B.P. Strong pedogenesis is documented during ~ 600 cal. years B.P., which weakened within 600–300 cal. BP and remained steady.
- Metal/Al ratios that indicate detrital influx, rather than chemical weathering indices like CIA and Rb/Sr ratio, are more suitable for reconstructing the past climate under tropical high rainfall conditions as in south-western India.

Supplementary Information The online version contains supplementary material available at https://doi.org/10.1007/s10498-021-09402-5.

Acknowledgements We thank Dr. V. Balaram, National Geophysical Research Institute, Hyderabad, Dr. J. N. Pattan and Dr. G. Parthiban, NIO, Goa, for providing access to and aiding in the ICP-MS measurements, and Dr. Balakrishna Kalluraya, Mangalore University, for access to acid digestion facility and Dr. K. V. Sujith for assistance.

Author's contributions KS collected the sediment cores, carried out analytical works and wrote the paper. AKW helped in the experiments and interpretation of the data. RS supervised the paper and helped in discussion and revision.

Funding KS thanks the University Grants Commission, New Delhi, for financial aid in the form of Junior and Senior Research Fellowships (F.17–109/98 (SA-I) dated 31/3/2005). AKW thanks the Council of Scientific and Industrial Research, New Delhi, for a senior research fellowship (9/449(035)2K8-EMR-I).

Data availability The dataset is available on request with the corresponding author.

Declarations

Conflict of interest The authors declare that they have no known competing financial interests that could have appeared to influence the work reported in this paper.

References

Amrutha K, Warrier AK, Sandeep K, Jyothinath A, Ananthapadmanabha AL, Shankar R (2021) Environmental magnetic properties of lateritic soils from Southwestern India. Eurasian Soil Sci 54(2):238–248

An Z, Clemens SC, Shen J, Qiang X, Jin Z, Sun Y, Prell WL, Luo J, Wang S, Xu H, Cai Y, Zhou W, Liu X, Liu W, Shi Z, Yan L, Xiao X, Chang H, Wu F, Ai L, Lu F (2011) Glacial–interglacial Indian summer monsoon dynamics. Science 333:719–723

Ananthapadmanabha AL, Shankar R, Sandeep K (2014) Rock magnetic properties of lateritic soil profiles from southern India: evidence for pedogenic processes. J Appl Geophys 111:203–210
Ao H, Deng C, Dekkers MJ, Sun Y, Liu Q, Zhu R (2010) Pleistocene environmental evolution in the Nihewan Basin and implication for early human colonization of North China. Quat Int 223–224:472–478
Babeesh C, Achyuthan H, Sajeesh TP (2018) Geochemical signatures of Karlad Lake Sediments, North Kerala: Source area weathering and provenance. J Geol Soc Ind 92:177–186
Babeesh C, Achyuthan H, Resmi M, Nautiyal CM, Shah RA (2019) Late-Holocene paleoenvironmental changes inferred from Manasbal Lake sediments, Kashmir Valley, India. Quat Int 507:156–171
Banerji US, Bhushan R, Joshi KB, Shaji J, Jull AJT (2021) Hydroclimate variability during the last two millennia from the mudflats of Diu Island, Western India. Geol J. https://doi.org/10.1002/gj.4116
Basu S, Anoop A, Sanyal P, Singh P (2017) Lipid distribution in the lake Ennamangalam, south India: indicators of organic matter sources and paleoclimatic history. Quat Int 443:238–247
Bertrand S, Hughen KA, Sepúlveda J, Pantoja S (2012) Geochemistry of surface sediments from the fjords of Northern Chilean Patagonia (44–47°S): spatial variability and implications for paleoclimate reconstructions. Geochim Cosmochim Acta 76:125–146
Bhattacharyya A, Sandeep K, Misra S, Shankar R, Warrier AK, Weijian Z, Zuefeng L (2015) Vegetational and climatic variations during the past 3100 years in southern India: evidence from Pollen, magnetic susceptibility and particle size data. Environ Earth Sci 74:3559–3572
Bhushan R, Sati SP, Rana N, Shukla AD, Mazumdar AS, Juyal N (2018) High-resolution millennial and centennial scale Holocene monsoon variability in the Higher Central Himalayas. Palaeogeogr Palaeoclimatol Palaeoecol 489:95–104
Brown ET, Le Callonnec L, German CR (2000) Geochemical cycling of redox sensitive metals in sediments from Lake Malawi, a diagnostic paleotracer for episodic changes in mixing depth. Geochim Cosmochim Acta 64:3515–3523
Das PK, Haake BG (2003) Geochemistry of Rewalsar Lake sediment, Lesser Himalaya, India: implications for source-area weathering, provenance and tectonic setting. Geosci J 7(4):299–312
Dearing JA, Dann RJL, Hay K, Lees JA, Loveland PJ, Maher BA (1996) Frequency-dependent susceptibility measurements of environmental materials. Geophys J Int 124:228–240
Felton AA, Russell JM, Cohen AS, Baker ME, Chesley JT, Lezzar KE, McGlue MM, Pigati JS, Quade J, Stager C, Tiercelin JJ (2007) Paleolimnological evidence for the onset and termination of glacial aridity from Lake Tanganyika, Tropical East Africa. Palaeogeogr Palaeoclimatol Palaeoecol 252: 405–423
Formoso MLL (2006) Some topics on geochemistry of weathering: a review. An Acad Bras Ciênc 78(4):809–820
Gopal V, Achyuthan H, Shah RA, Jayaprakash M (2020) Physicochemical characteristics and spatial distribution pattern of the Yercaud Lake surface sediments. South India Geol J. https://doi.org/10.1002/gj.4023
Jin Z, Wang S, Ji S, Zhang E, Ji J, Li F (2001a) Weak chemical weathering during the Little Ice Age recorded by lake sediments. Sci China (series d) 44(7):652–658
Jin Z, Wang S, Shen J, Zhang E, Li F, Ji J, Lu X (2001b) Chemical weathering since the little ice age recorded in lake sediments: a high resolution proxy of past climate. Earth Surf Process Landf 26:775–782
Jin Z, Li F, Cao J, Wang S, Yu J (2006) Geochemistry of Daihai Lake sediments, Inner Mongolia, north China: implications for provenance, sedimentary sorting, and catchment weathering. Geomorphology 80:147–163
Liu J, Chen J, Selvaraj K, Xu Q, Wang Z, Chen F (2014) Chemical weathering over the last 1200 years recorded in the sediments of Gonghai Lake, Lvliang Mountains, North China: a high-resolution proxy of past climate. Boreas. 101111/bor12072 ISSN 0300–9483.
Lone AM, Achyuthan H, Shah RA, Sangode SJ, Kumar P, Chopra S, Sharma R (2020) Paleoenvironmental shifts spanning the last ~6000 years and recent anthropogenic controls inferred from a high-altitude temperate lake: Anchar Lake. NW Himalaya Holocene 30(1):23–36
Mackereth FJH (1966) Some chemical observations on post-glacial lake sediments. Philos Trans R Soc Lond B 250:165–213
Maher BA, Taylor RM (1988) Formation of ultrafine-grained magnetite in soils. Nature 336:368–370
Maher BA, Thompson R (1991) Mineral magnetic record of the Chinese loess and paleosols. Geology 19:3–6
McLennan SM (1989) Rare earth elements in sedimentary rocks: influence of provenance and sedimentary processes. Rev Mineral Geochem 21:170–199
Mehra OP, Jackson ML (1960) Iron oxide removal from soils and clays by a dithionite-citrate system buffered with sodium bicarbonate. Clays Clay Miner 7:317–327

Minyuk PS, Borkhodoev VY, Wennrich V (2014) Inorganic geochemistry data from Lake El'gygytgyn sediments: marine isotope stages 6–11. Clim past 10:467–485
Miriyala P, Sukumaran NPP, Nath BNN, Ramamurty PBB, Sijinkumar AVV, Vijayagopal B, Ramaswamy V, Sebastian T (2017) Increased chemical weathering during the deglacial to mid-Holocene summer monsoon intensification. Sci Rep 7:44310
Mischke S, Zhang CJ (2010) Holocene cold events on the Tibetan Plateau. Glob Planet Change 72:155–163
Mishra PK, Ankit Y, Gautam PK, Lakshmidevi CG, Singh P, Anoop A (2019) Inverse relationship between South-West and North-East Monsoon during the late Holocene: geochemical and sedimentological record from Ennamangalam Lake, Southern India. Catena 182:104117
Nair V, Achyuthan H (2017) Geochemistry of Vellayani lake sediments: indicators of weathering and provenance. J Geol Soc Ind 89:21–26
Pattan JN, Masuzawa T, Yamamoto M (2005) Variations in terrigenous sediment discharge in a sediment core from southeastern Arabian Sea during the last 140 ka. Curr Sci 89(8):1421–1425
Rajmanickam V, Achyuthan H, Eastoe C, Farooqui A (2017) Early-Holocene to present palaeoenvironmental shifts and short climate events from the tropical wetland and lake sediments, Kukkal Lake. South India Geochem Palynol Holoc 27(3):404–417
Sandeep K, Warrier AK, Harshavardhana BG, Shankar R (2012) Rock magnetic investigations of surface and sub–surface soil samples from five Lake Catchments in Tropical Southern India. Int J Environ Res 6(1):1–18
Sandeep K, Shankar R, Warrier AK, Weijian Z, Xuefeng L (2015) The environmental magnetic record of palaeoenvironmental variations during the past 3100 years: A possible solar influence? J Appl Geophys 118:24–36
Shah RA, Achyuthan H, Lone MA (2020a) Holocene palaeoenvironmental records from the high-altitude Wular Lake, Western Himalayas. Aquat Geochem 26:31–52
Shah RA, Achyuthan H, Lone MA, Kumar S, Kumar P, Sharma R, Amir M, Singh AK, Dash C (2020b) Holocene palaeoenvironmental records from the high-altitude Wular Lake. Western Himalayas Holocene 30(5):733–743
Shah RA, Achyuthan H, Lone A, Kumar P, Ali A, Rahman A (2021) Palaeoenvironment shifts during last ~ 500 years and eutrophic evolution of the Wular Lake, Kashmir Valley, India. Limnology 22:111–120
Sinha R, Smykatz-Kloss W, Stüben D (2006) Late Quaternary palaeoclimatic reconstruction from the lacustrine sediments of the Sambhar playa core, Thar Desert margin, India. Palaeogeogr Palaeoclimatol Palaeoecol 233:252–270
Sun Y, Wu F, Clemens SC, Oppo DW (2008) Processes controlling the geochemical composition of the South China Sea sediments during the last climatic cycle. Chem Geol 257:243–249
Sun QL, Wang SM, Zhou J, Chen ZY, Shen J, Xie XP, Wu F, Chen P (2010) Sediment geochemistry of Lake Daihai, north-central China, implications for catchments weathering and climate change during the Holocene. J Paleolimnol 43:75–87
Sun W, Zhang E, Liu E, Chang J, Ji S (2018) Impacts of chemical weathering and grain-size distribution on Lake Xingkai sediment geochemistry since the last interglacial period. Palaeogeogr Palaeoclimatol Palaeoecol 512:71–79
Taylor RM, Maher BA, Self PG (1987) Magnetite in soils: I. The synthesis of singledomain and superparamagnetic magnetite. Clay Miner 22:411–422
USGS (1995) United States Geological Survey, Certificate of Analysis—MAG-1 and SCo-1 USGS, Denver, Colorado
Veena MP, Achyuthan H, Eastoe C, Farooqui A (2014) Human impact on low-land Vellayani Lake, south India: a record since 3000 yrs BP. Anthropocene 8:83–91
Vidic NJ, TenPas JD, Verosub KL, Singer MJ (2000) Separation of pedogenic and lithogenic components of magnetic susceptibility in the Chinese loess/palaeosol sequence as determined by the CBD procedure and a mixing analysis. Geophys J Int 142:551–562
Warrier AK, Shankar R (2009) Geochemical evidence for the use of magnetic susceptibility as a paleorainfall proxy in the tropics. Chem Geol 265:553–562
Warrier AK, Sandeep K, Shankar R (2017) Climatic periodicities recorded in a lake sediment magnetic susceptibility data: further evidence for solar forcing on the Indian Summer Monsoon. Geosci Front 8(6):1349–1355
Wei GJ, Li XH, Liu Y, Shao L, Liang XR (2006) Geochemical record of chemical weathering and monsoon climate change since the early Miocene in the South China Sea. Paleoceanography 21(4):1–11

Xu QH, Chen FH, Zhang SR, Cao XY, Li JY, Li YC, Li MY, Chen JH, Liu JB, Wang ZL (2016) Vegetation succession and East Asian summer monsoon changes since the last deglaciation inferred from high-resolution pollen record in Gonghai Lake, Shanxi Province. China Holocene 27(6):835–846

Zhong W, Pen Z, Xue J, Ouyang J, Tang X, Cao J (2012) Geochemistry of sediments from Barkol Lake in the westerly influenced northeast Xinjiang: implications for catchment weathering intensity during the Holocene. J Asian Earth Sci 50:7–13